

# Sensitivity Enhancement of Third-order Nonlinearity Measurement in THz Frequency Range

A. Nabilkova, A. Ismagilov, M. Melnik, M. Zhukova, M. Guselnikov, S. Kozlov, A. Tcypkin

**Abstract**—In this article for the first time we applied the eclipse Z-scan technique which is by one order of magnitude more sensitive than the conventional Z-scan technique to measure LiNbO<sub>3</sub> crystal's nonlinear refractive index in the THz range. The obtained value of LiNbO<sub>3</sub> nonlinear refractive index is estimated to be  $5 \pm 2 \times 10^{-11} \text{ cm}^2/\text{W}$  which is commensurate with known results. This value correlates with the theoretically calculated nonlinear refractive index coefficient of vibrational nature. The influence of thermal nonlinearity on the experimental results can be neglected, since the estimated temperature induced refractive index change  $\Delta n_T$  equals to  $2.6 \times 10^{-5}$ , while addition  $\Delta n_{nl}$  from optical nonlinearity is  $2.9 \times 10^{-3}$ . The demonstrated heightened sensitivity of eclipse Z-scan allows to hold promise for the properties evaluation of materials exhibiting lower nonlinear refractive indices, thus expanding its applicability in characterizing diverse nonlinear optical materials.

**Index Terms**—Article submission, IEEE, IEEEtran, journal, LATEX, paper, template, typesetting.

## I. INTRODUCTION

NONLINEAR characteristics of materials such as nonlinear refractive index ( $n_2$ ) and absorption coefficients in the terahertz (THz) frequency range have already been experimentally and theoretically investigated for a number of liquids [1]–[5], vapors [4], [6], [7] and crystals [8]–[15]. Within the existing amount of work, the experimental method for determining the value of  $n_2$  is used along with theoretical approach [1], [2], [16] to prove the validity of the theory [17] and stimulate the development of fundamental research for the evaluation of the coefficient  $n_2$  [8], [18].

Besides, various experimental techniques are used to investigate nonlinear properties of materials in the THz range, each with its unique setup and specific objectives. Examples of such techniques include: Z-scan [19]–[23], widely employed for nonlinearities extraction across all spectral ranges, 4f-system Z-scan [24]–[26], pump-probe with time delay [10], [27]–[30], four wave mixing [31], nonlinear ellipse rotation [32], [33], and full-phase analysis [4]. These techniques primarily leverage self-induced lensing phenomena to explore and quantify the nonlinear properties of materials.

It is important to note the orders of magnitude of previously measured and estimated nonlinear refractive indices. For

liquids, these values are of the order of  $10^{-10}$ – $10^{-9} \text{ cm}^2/\text{W}$  [1], [23], [34], for solids these values vary from  $10^{-13} \text{ cm}^2/\text{W}$  to  $10^{-11} \text{ cm}^2/\text{W}$  [35]–[37]. In particular, for lithium niobate (LiNbO<sub>3</sub>) crystal the value of  $n_2$  in the terahertz region is deduced to be  $10^{-11} \text{ cm}^2/\text{W}$  [38], [39].

The described nonlinearities for solids are couple orders of magnitude lower than for liquids. The sensitivity of the conventional laboratory tabletop Z-scan setup [2] becomes insufficient for the comprehensive investigation of the nonlinearities that possessed by solids. In particular, the robust interferometric sensitivity characteristic of the Z-scan method, which facilitates the determination of alterations in transmittance due to phase change, emanates from the interference (diffraction) effects engendered by distinct segments of the spatial profile within the far field [19].

Only a few unique techniques, such as one consisting of single-mode Fabry-Pérot microcavity with detection by phase contrast imaging technique using a 4f system [15] or high-powered sources like FEL [40], are suitable for evaluating nonlinear refractive index  $n_2$  of LiNbO<sub>3</sub> in the THz range. Another technique is based on the phenomenon of third harmonic generation disappearing during single-cycle THz pulse propagation in cubic nonlinear medium. It is replaced by the generation of radiation at quadruple frequencies and by the position of the dip in the region of triple frequencies and the peak of quadruple frequency it is possible to evaluate the nonlinear refractive index of LiNbO<sub>3</sub> [39].

One of the alternative method to increase sensitivity of the conventional Z-scan measurements is the eclipse Z-scan [41], [42]. The system's sensitivity is enhanced by selectively registering signal counts within the beam peripheries. This is achieved through the obstruction of the central region due to implying disk aperture that mask the central segment of the laser beam. The higher sensitivity to transmission variations derives from the manner light bypasses the obstructing disk, thereby enabling the detection of an "eclipse" and facilitating assessments of the third-order optical nonlinearity inherent in materials. Notably, the application of the eclipse Z-scan method in the context of the THz frequencies represents a novel endeavor, necessitating adaptations to accommodate this spectral domain.

In this work we introduce an advancement in measuring the third-order nonlinearity in the THz spectral range with eclipse Z-scan method. With a one-order sensitivity enhancement over conventional Z-scan techniques, this approach has yielded a remarkable LiNbO<sub>3</sub> nonlinear refractive index value of  $5 \pm 2 \times 10^{-11} \text{ cm}^2/\text{W}$ . The observed value of the refractive index change induced by temperature variations ( $\Delta n_T$ ), estimated as

This paper was produced by the IEEE Publication Technology Group. They are in Piscataway, NJ.

Manuscript received April 19, 2021; revised August 16, 2021. Corresponding author is A. Tcypkin.

A. Nabilkova, A. Ismagilov, M. Melnik, M. Zhukova, M. Guselnikov, S. Kozlov, A. Tcypkin are with Research and Education Center of Photonics and Optical IT, ITMO University (e-mail: tcypkinan@itmo.ru)

$2.6 \times 10^{-5}$ , and the dominant refractive index change ( $\Delta n_{nl}$ ) attributed to optical nonlinearity, measured as  $2.9 \times 10^{-3}$ , assume that the observed nonlinear behavior cannot arise from thermal effects. It could be stated that the nonlinearity obtained has a vibrational nature, since the value obtained coincides with the value theoretically calculated earlier [1], [36] according to the analytical model [8]. In addition, a comparative analysis of the sensitivities of the conventional and eclipse Z-scan techniques is presented, offering insights into their capabilities.

## II. EXPERIMENT

With a view to reach an order-of-magnitude enhancement of the signal-to-noise ratio of the conventional Z-scan technique, the disk [42], [43] instead of the aperture is implemented into setup according to pioneering works in mentioned direction [19], [41]. The application of the disk allows using both open and closed aperture geometry in the same way as aperture does. Here, the nonlinear refractive index  $n_2$  of lithium niobate is experimentally determined utilizing the eclipse Z-scan technique in conjunction with a pulsed THz radiation source.

The experimental setup is illustrated in Fig. 1. The THz source operates at a repetition rate of 1 kHz. The vertically polarized THz pulse displays a duration of 1 ps, a pulse energy of 400 nJ (with a peak electric field strength of 0.27 MV/cm), and a spectral range extending from 0.1 to 2.5 THz [1]. The full width at half maximum (FWHM) of the collimated THz beam is determined using the knife-edge method, yielding values of 8.5 mm for the x-axis and 5.6 mm for the y-axis, as reported in [1]. The beam is tightly focused onto the sample via the PM1 mirror (the focal length of the parabolic PM1 mirror is 12.7 mm), resulting in a beam diameter of approximately 1.5 mm at the focal point. The beam diameter values are verified by the knife-edge method with a precision of 100  $\mu\text{m}$ . The peak intensity at focus reaches  $0.5 \times 10^8 \text{ W/cm}^2$ . Then the THz radiation is collimated by the parabolic mirror PM2 and focused by the lens with focal length of 50 mm. The slight ellipticity of the beam observed in the experiment should not impact the closed aperture Z-scan traces [44]. The metal disk is installed in front of the lens. The diameter of disk is selected relative to the required sensitivity of the eclipse Z-scan technique. Detection is performed using a bolometer (Gentec-EO THZ5B-BL-DZ-D0).

## III. RESULTS

### A. Experimental data of eclipse Z-scan

In order to conduct a comparative analysis of the experimental curves obtained with the eclipse Z-scan and conventional Z-scan methods, the 10% transmittance disk was replaced with a 2% transmittance aperture. Fig. 2 (a) shows unnormalized closed aperture Z-scan and eclipse Z-scan (EZ-scan) curves obtained experimentally. Fig 2 (b) presents results of the open aperture measurements, which were carried out without disk to exclude the influence of the material's absorption properties. It can be seen that the amplitude of the Z-scan curve fluctuations, where the peak and valley should be, is comparable to the noise of the curves for the EZ-scan. Notably, the difference

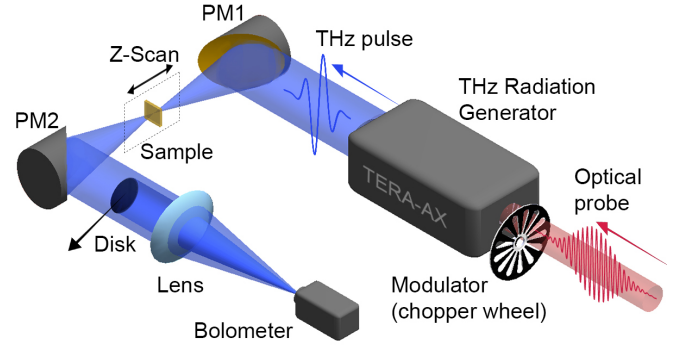


Fig. 1. Experimental setup for the eclipse Z-scan measurements. The THz pulse is produced through optical rectification within a MgO:LiNbO<sub>3</sub> crystal (Tera-AX Avesta project [45]), sourced from a 35 femtosecond duration pulse with a central wavelength of 790 nm and a pulse energy of 1 mJ originating from a Ti:Sapphire femtosecond laser with a regenerative amplifier (Regulus Avesta project). Parabolic mirrors (PM1, PM2) are used to focus and collimate the THz pulse. The modulator is used to synchronize the bolometer and the THz radiation source. The disk can be moved from the beam to the open position. A bolometer (Gentec-EO THZ5B-BL-DZ-D0) is used to measure the power of THz radiation.

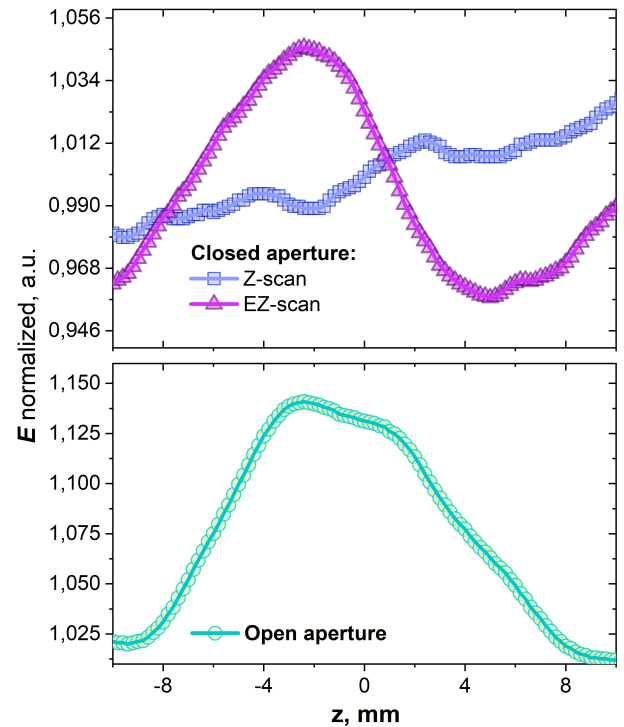


Fig. 2. (a) Comparison of the experimental results from closed aperture measurement of Z-scan and eclipse Z-scan (EZ-scan). All obtained curves are normalized to the corresponding mean value to show the difference between  $\Delta T$  and order of sensitivity boosted. (b) Experimental results for the case of open aperture measurements without disk.

between the peak to valley in the field  $E$  registered here for the EZ-scan curves is more than 10 times greater than for the conventional Z-scan curves.

Fig 3 shows the experimental results of the closed aperture eclipse Z-scan (EZ-scan) measurements normalized to open aperture measurements, compared to the analytical modeling

of the EZ-scan. As can be seen in Fig. 2 (a) and 3, the ends of the curve point upward may be an analytical artifact arising from dividing the closed aperture curve by the open aperture curve due to the presence of noise in both curves.

These experimental results demonstrate that the difference between the normalized peak and valley transmittance  $\Delta T$  is found to be 0.021. Thus, using the empirical linear relationship between  $\Delta T$  and nonlinear phase shift  $\Delta\Phi_0$  [41], [42] we can extract the nonlinear refractive index  $n_2$  of LiNbO<sub>3</sub> crystal by following equation:

$$n_2 = \frac{\Delta T}{0.68I_{in}} \times \frac{(1-S)^{0.44}}{kL_\alpha} \quad (1)$$

Substituting the experimentally obtained value of  $\Delta T$  we found  $n_2 = 5 \pm 2 \times 10^{-11} \text{ cm}^2/\text{W}$ .

### B. Theoretical model of eclipse Z-scan

The convenience and precision of applying mathematical expressions [19] for the THz range and pulsed few-cycle radiation have already been shown [1], [2], [21]. In our simulations, the field distribution  $E$  assuming a TEM<sub>00</sub> Gaussian beam of waist radius  $w_0$  traveling in the  $+z$  direction is given by:

$$E(r, t, z) = E_0(t) \frac{w_0}{w(z)} \exp\left(\frac{-r^2}{w(z)^2} - \frac{ikr^2}{2R(z)}\right) e^{-i\phi(r,t,z)} \quad (2)$$

where  $E_0(t)$  is the initial temporal envelope of the input field  $E_0 \sin(2\pi\nu_0 t)$ ,  $w(z)^2 = w_0^2(1 + z^2/z_0^2)$  is the beam radius,  $R(z) = z(1 + z^2/z_0^2)$  is the radius of curvature of the wave front at  $Z$ ,  $z_0 = kw_0^2/2$  is the diffraction length of the beam, and  $k = 2\pi/\lambda$  is the wave vector. The  $e^{-i\phi(r,t,z)}$  term contains all the radially uniform phase variations. In the thin sample slowly varying envelope approximation, the electric field amplitude only changes due to the absorption, while the phase of the electric field due to the nonlinear refraction resulting in nonlinear phase term  $e^{-i\Delta\phi(r,t,z)}$ . Gaussian decomposition (GD) method is implemented according to [19] to calculate the complex field distribution  $E_a$  in the aperture plane. So  $E_a$  is derived as:

$$E_a(r, t, z) = E(z, t) \exp(-\alpha L/2) \times \sum_{m=0}^{+\infty} \frac{[-i\Delta\phi_0(z, t)]^m}{m!} \frac{w_{m0}}{w_m} \exp\left(\frac{-r^2}{w_m^2} - \frac{ikr^2}{2R_m} + iQ_m\right) \quad (3)$$

where  $\Delta\phi_0(z, t) = \Delta\Phi_0(t)/(1 + z^2/z_0^2)$ ,  $\Delta\Phi_0(t) = k\Delta n_0(t)L$  is the nonlinear phase shift. The GD method involves decomposing of the electric field at the sample exit plane into Gaussian beams using a Taylor series expansion of the nonlinear phase term. This approach is based on the assumption of small phase changes, allowing to take into consideration only the initial terms of the expansion. Therefore, defining  $d$  as the propagation distance in free space from the sample to the disk, and  $g = 1 + d/R(z)$ , other parameters in Eq. 3 according to [19] are expressed as:

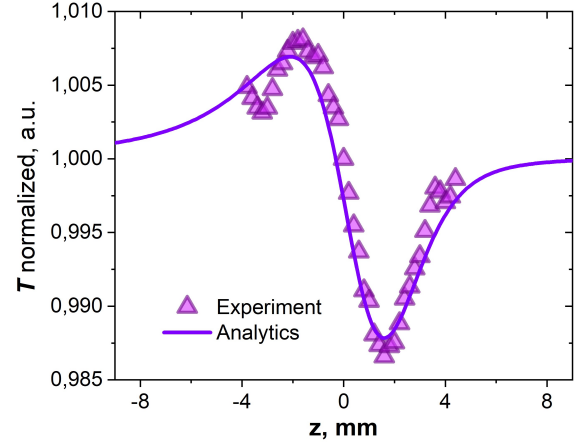


Fig. 3. Comparison of the experimental results of the Z-scan method for the pulsed broadband THz radiation for the LiNbO<sub>3</sub> crystal with an analytical Z-scan curve. The analytical curve is calculated using Eq. 10.

$$w_{m0}^2 = w_z^2/(2m+1) \quad (4)$$

$$d_m = kw_{m0}^2/2 \quad (5)$$

$$w_m^2 = w_{m0}^2 (g^2 + d^2/d_m^2) \quad (6)$$

$$R_m = d \left(1 - \frac{g}{g^2 + d^2/d_m^2}\right)^{-1} \quad (7)$$

$$\theta_m = \tan^{-1} \left(\frac{d/d_m}{g}\right) \quad (8)$$

The transmitted through the disk power is obtained by spatially integrating  $E_a(r, t, z)$  from the disk radius  $r_d$  to the beam radius on the aperture  $w_a$  giving:

$$P_T(\Delta\Phi_0(t)) = c\epsilon_0 N_0 \pi \int_{r_d}^{w_a} |E_a(r, t)|^2 r dr \quad (9)$$

Integrating up to beam radius on the aperture  $w_a$  allows neglecting the impact of "noise", where the beam profile fluctuates around zero. Thus, the normalized transmittance can be calculated as

$$T(z) = \frac{\int_{-\infty}^{+\infty} P_T(\Delta\Phi_0(t)) dt}{S \int_{-\infty}^{+\infty} P_i(t) dt} \quad (10)$$

where  $P_i(t) = \pi w_0^2 I_0(t)/2$  is the instantaneous input power (within the sample),  $S = 1 - \exp(-2r_d^2/w_a^2)$  is the disk linear transmittance.

By gathering the setup parameters and the beam characteristics from the experiment, the nonlinear refractive index  $n_2$  value calculated from 1, and substituting them into equation 10 (and nested equations), we can obtain the normalized transmittance  $T$  from the coordinates of crystal displacement  $z$ . Fig. 4 shows a comparison of analytical eclipse and conventional Z-scan curves, demonstrating the order of sensitivity enhancement for the former method. The Z-scan curves are obtained with the same theoretical model, however Eq. 9 is adjusted to perform integration over the aperture: from 0 to  $r_a$ .

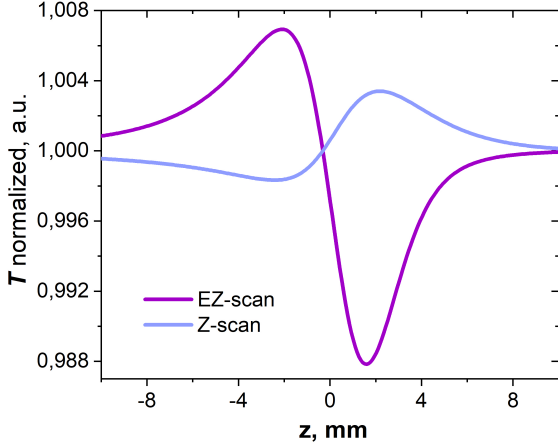


Fig. 4. Comparison of the analytical results of the Z-scan and eclipse Z-scan (EZ-scan) modeling.

#### IV. DISCUSSION

The experimental as well as the analytical findings underscore the efficiency of employing eclipse Z-scan instead of conventional Z-scan method, culminating in an enhancement in the sensitivity of THz systems by an order of magnitude. The achieved order of nonlinearity, approximately  $10^{-11}$   $\text{cm}^2/\text{W}$ , stands as a noteworthy accomplishment. As was mentioned, the diameter of the metal disk, which determines the parameter  $S$ , was chosen on the basis of two considerations: the sensitivity of the eclipse Z-scan method and the sensitivity of the detector. As a result, a disk with a diameter that covers 90% of the incident radiation was chosen, which allowed us to perform measurements with a signal-to-noise ratio of 10 and to obtain a significant drop in the Z-scan curve.

Certain types of light sources can induce cumulative interactions, such as pulsed THz systems with large pulse durations or high repetition rates. In such systems, thermal effects may occur. In the context of determining the nonlinear refractive index of liquids [1]–[3], temperature-induced nonlinear effects were deemed negligible, as each pulse interact with a refreshed surface of liquid jet. However, for crystals, consideration of temperature fluctuations during the experiment becomes mandatory for a comprehensive evaluation of their influence on the refractive index. Strong thermal effects can contribute to the refractive index by inducing temperature fluctuations through non-radiative interactions within the system. The upper bound evaluation was made for temperature nonlinear refractive index contribution  $n_{2T}$  in comparison with the contribution of vibrational nonlinear refractive index  $n_{2nl}$  to the change in the refractive index  $\Delta n$ .

To estimate the thermal effects per laser repetition rate, we use the following expression  $n_{2th} = \frac{dn}{dT} \frac{\alpha R^2}{\kappa}$  [46]. Here  $\frac{dn}{dT}$  displays the speed of refractive index change with temperature variation, it is found to be  $7.03 \times 10^{-4}$   $1/\text{K}$  [9].  $\alpha = 9$   $\text{cm}^{-1}$  denotes the linear absorption coefficient of the material,  $\kappa = 0.046$   $\text{W}/(\text{cm} \times \text{K})$  stands for the thermal conductivity, and  $R = 0.7$   $\text{mm}$  is a radius of a circular laser beam in focus.

The response time  $\tau_r$  for the thermal nonlinearity is given by  $\tau_r \approx \frac{\rho C R^2}{\kappa}$  [47], so thermally induced  $\Delta n$  per one repetition of pulses would be  $\frac{n_{2th} I \tau_p}{\tau_r}$ , because interaction of the crystal with the beam occurs for about pulse duration  $\tau_p$ , which is equal to 1 ps. Here, material's density  $\rho$  is  $4700$   $\text{kg}/\text{m}^3$ , heat capacity  $C$  is  $628$   $\text{J}/(\text{kg K})$ .

The energy per one repetition can be estimated as  $Q = \epsilon P m$ , where pulse energy  $P$  is equal to  $400$   $\text{nJ}$ , emissivity of the crystal  $\epsilon$  is  $0.6$ , and number of pulses per one repetition  $m$ , controlled by chopper's speed, is  $40$ . If we assume that all obtained energy is used for heating, then the crystal heats up according to the equation  $\Delta T_h = \frac{Q}{C m}$ , where  $m = \rho \pi R^2 L$  is mass of illuminated area of the crystal. Then, during the time when the chopper closes the laser, the crystal cools by an amount  $\Delta T_c = \frac{\tau_h S \Delta T_h}{m C}$ , where  $S$  is an illuminated area and  $h$  is a heat transfer coefficient equal to  $10$   $\text{W}/(\text{m}^2 \text{K})$ . Accordingly, the temperature  $\Delta T$  to which the crystal is heated during one passage will be equal to  $\Delta T_h - \Delta T_c$ . The overall heating temperature of the sample for the entire duration of the experiment is  $0.1 \times 10^{-3}$   $\text{K}$ .

As an upper estimate, we assume that the temperature change  $\Delta T$  is constant while the spot size of the laser beam on the crystal should change as the sample is displaced through the beam focus in the  $z$  direction. The sample passes this path in 10 seconds, so the crystal has time to interact with radiation and heat up by  $\Delta T$  in 250 repetitions, according to repetition rate of laser and frequency of chopper. Therefore, accumulative thermal contribution to refractive index change  $\Delta n_{th}$  is  $2.6 \times 10^{-5}$ , while contribution of vibrational nonlinearity  $\Delta n_{nl}$  is  $2.9 \times 10^{-3}$ .

#### V. CONCLUSION

This study shed a light on an adjustment to tried and tested in THz range Z-scan technique, that offer to gain sensitivity of experiment. Eclipse Z-scan methodology was used for assessing third-order nonlinearity within the THz spectral domain. Demonstrating a sensitivity enhancement of one order compared to conventional Z-scan methodologies [1], [2], our refinement has unveiled a noteworthy nonlinear refractive index value  $n_2$  for  $\text{LiNbO}_3$  crystal of  $5 \pm 2 \times 10^{-11}$   $\text{cm}^2/\text{W}$ . Additionally, the theoretical approach, that describes the behavior of light in a crystal when conducting eclipse Z-scan measurement, was modified to justify the obtained value of  $n_2$ . Our results show that experimentally obtained Z-scan measurement curves and simulations of self-focusing processes in  $\text{LiNbO}_3$  crystal are in good agreement. Notably, our investigation into temperature-induced variations in refractive index ( $\Delta n_T$ ), estimated as  $2.6 \times 10^{-5}$ , alongside the predominant refractive index change ( $\Delta n_{nl}$ ) attributed to optical nonlinearity, measured at  $2.9 \times 10^{-3}$ , suggests that the observed nonlinear phenomena mostly ascribed to optical nature. This assertion is supported by the congruence between our measured nonlinearity and previously theorized values [1], [36], as predicted by the analytical framework proposed by [8], indicating a vibrational underpinning to the observed nonlinear behavior. Furthermore, a comparative evaluation of the sensitivities inherent to conventional and eclipse Z-scan

methods is provided experimentally and analytically, affording valuable insights into their respective efficiency and potential applications.

The results presented emphasize the importance of exploring the nonlinear refractive index of diverse media to identify materials exhibiting high nonlinearity, thereby facilitating the advancement of nonlinear terahertz optics. The nonlinear refractive index plays a pivotal role in determining the optical response of materials, enabling the manipulation of light for various applications in photonics and optoelectronics. Devices such as semiconductor optical amplifiers, flip-flops, switchers, optical transistors, and modulators have been identified as examples of systems with high nonlinear refractive index, showcasing the practical relevance of investigating this property. By exploring and harnessing the nonlinear refractive index of materials, researchers can unlock new avenues for enhancing the performance and functionality of optical devices. This research not only contributes to expanding our fundamental understanding of light-matter interactions but also holds immense promise for driving innovation in the field of nonlinear optics, for example, developing devices for creating all-optical computer.

#### ACKNOWLEDGMENTS

All authors acknowledge support from the Russian Science Foundation (Grant No. 24-22-00084).

#### REFERENCES

- [1] A. Tcypkin, M. Zhukova, M. Melnik, I. Vorontsova, M. Kulya, S. Putilin, S. Kozlov, S. Choudhary, and R. W. Boyd, "Giant third-order nonlinear response of liquids at terahertz frequencies," *Physical Review Applied*, vol. 15, no. 5, p. 054009, 2021.
- [2] A. N. Tcypkin, M. V. Melnik, M. O. Zhukova, I. O. Vorontsova, S. E. Putilin, S. A. Kozlov, and X.-C. Zhang, "High kerr nonlinearity of water in thz spectral range," *Optics express*, vol. 27, no. 8, pp. 10419–10425, 2019.
- [3] F. Novelli, C. Y. Ma, N. Adhlakha, E. M. Adams, T. Ockelmann, D. Das Mahanta, P. Di Pietro, A. Perucchi, and M. Havenith, "Nonlinear terahertz transmission by liquid water at 1 thz," *Applied Sciences*, vol. 10, no. 15, p. 5290, 2020.
- [4] K. J. G. Francis, M. L. P. Chong, E. Yiwen, and X.-C. Zhang, "Terahertz nonlinear index extraction via full-phase analysis," *Optics Letters*, vol. 45, no. 20, pp. 5628–5631, 2020.
- [5] S.-j. Guo, C.-j. Ruan, D.-y. Kong, J. Dai, Y. Zhang, and W.-l. He, "Research on terahertz transmission characteristics of nonpolar liquid based on frequency-domain spectroscopy," *JOSA B*, vol. 37, no. 7, pp. 1942–1947, 2020.
- [6] P. Rasekh, A. Safari, M. Yildirim, R. Bhardwaj, J.-M. Menard, K. Dolgaleva, and R. W. Boyd, "Terahertz nonlinear spectroscopy of water vapor," *Acs Photonics*, vol. 8, no. 6, pp. 1683–1688, 2021.
- [7] K. Johnson, M. Price-Gallagher, O. Mamer, A. Lesimple, C. Fletcher, Y. Chen, X. Lu, M. Yamaguchi, and X.-C. Zhang, "Water vapor: an extraordinary terahertz wave source under optical excitation," *Physics Letters A*, vol. 372, no. 38, pp. 6037–6040, 2008.
- [8] K. Dolgaleva, D. V. Materikina, R. W. Boyd, and S. A. Kozlov, "Prediction of an extremely large nonlinear refractive index for crystals at terahertz frequencies," *Physical Review A*, vol. 92, no. 2, p. 023809, 2015.
- [9] R. Sowade, I. Breunig, C. Tulea, and K. Buse, "Nonlinear coefficient and temperature dependence of the refractive index of lithium niobate crystals in the terahertz regime," *Applied Physics B*, vol. 99, pp. 63–66, 2010.
- [10] S. Zibod, P. Rasekh, M. Yildirim, W. Cui, R. Bhardwaj, J.-M. Menard, R. W. Boyd, and K. Dolgaleva, "Strong nonlinear response in crystalline quartz at thz frequencies," *Advanced Optical Materials*, vol. 11, no. 15, p. 2202343, 2023.
- [11] M. Zhukova, M. Melnik, I. Vorontsova, A. Tcypkin, and S. Kozlov, "Estimations of low-inertia cubic nonlinearity featured by electro-optical crystals in the thz range," in *Photonics*, vol. 7, no. 4. MDPI, 2020, p. 98.
- [12] M. Jazbinsek, U. Puc, A. Abina, and A. Zidansek, "Organic crystals for thz photonics," *Applied Sciences*, vol. 9, no. 5, p. 882, 2019.
- [13] A. Woldegeorgis, T. Kurihara, B. Beleites, J. Bossert, R. Grosse, G. G. Paulus, F. Ronneberger, and A. Gopal, "Thz induced nonlinear effects in materials at intensities above 26 gw/cm<sup>2</sup>," *Journal of Infrared, Millimeter, and Terahertz Waves*, vol. 39, pp. 667–680, 2018.
- [14] M. S. Guselnikov, M. O. Zhukova, and S. A. Kozlov, "Media for ultrafast thz photonics," *Optics and Spectroscopy*, vol. 131, no. 2, pp. 268–276, 2023.
- [15] Y. Huang, Y. Lu, W. Li, X. Xu, X. Jiang, M. Ruobin, L. Chen, N. Ruan, Q. Wu, and J. Xu, "Giant kerr nonlinearity of terahertz waves mediated by stimulated phonon polaritons in a microcavity chip," *Light: Science & Applications*, 12 2023.
- [16] T. Amini and F. Jahangiri, "Regenerative terahertz wave parametric amplifier based on four-wave mixing in asynchronously pumped graphene oxide integrated topas," *Optics Express*, vol. 29, no. 21, pp. 33053–33066, 2021.
- [17] A. Nabilkova, A. Ismagilov, M. Melnik, A. Tcypkin, M. Guselnikov, S. Kozlov, and X.-C. Zhang, "Controlling water giant low-inertia nonlinear refractive index in the thz frequency range via temperature variation," *Optics Letters*, vol. 48, no. 5, pp. 1312–1314, 2023.
- [18] M. A. Hemmatian and F. Jahangiri, "A simplified model for predicting the nonlinear properties of water and centrosymmetric media at terahertz frequencies," *Optical and Quantum Electronics*, vol. 55, no. 4, p. 359, 2023.
- [19] M. Sheik-Bahae, A. A. Said, T.-H. Wei, D. J. Hagan, and E. W. Van Stryland, "Sensitive measurement of optical nonlinearities using a single beam," *IEEE journal of quantum electronics*, vol. 26, no. 4, pp. 760–769, 1990.
- [20] E. W. Van Stryland and M. Sheik-Bahae, "Z-scan," in *Characterization techniques and tabulations for organic nonlinear optical materials*. Routledge, 2018, pp. 671–708.
- [21] M. Melnik, I. Vorontsova, S. Putilin, A. Tcypkin, and S. Kozlov, "Methodical inaccuracy of the z-scan method for few-cycle terahertz pulses," *Scientific reports*, vol. 9, no. 1, p. 9146, 2019.
- [22] W.-Q. He, C.-M. Gu, and W.-Z. Shen, "Direct evidence of kerr-like nonlinearity by femtosecond z-scan technique," *Optics Express*, vol. 14, no. 12, pp. 5476–5483, 2006.
- [23] H. Zhao, Y. Tan, Y. Zhao, M. Liu, and L. Zhang, "Terahertz nonlinear spectroscopy of liquid water," *IEEE Transactions on Terahertz Science and Technology*, vol. 14, no. 1, pp. 76–81, 2024.
- [24] G. Boudebs, V. Besse, C. Cassagne, H. Leblond, and C. B. de Araújo, "Nonlinear characterization of materials using the d4&#x3c3; method inside a z-scan 4f-system," *Opt. Lett.*, vol. 38, no. 13, pp. 2206–2208, Jul 2013. [Online]. Available: <https://opg.optica.org/ol/abstract.cfm?URI=ol-38-13-2206>
- [25] Z. Li and Y. Song, "Characterizing the nonlinear optical properties of 2d materials by double 4f nonlinear imaging system with phase object and four-wave-mixing microscopy," *Two-Dimensional Materials for Nonlinear Optics: Fundamentals, Preparation Methods, and Applications*, pp. 87–102, 2024.
- [26] H. Wang, C. Ciret, J.-L. Godet, C. Cassagne, and G. Boudebs, "Measurement of the optical nonlinearities of water, ethanol and tetrahydrofuran (thf) at 355 nm," *Applied Physics B*, vol. 124, pp. 1–6, 2018.
- [27] A. O. Nabilkova, M. O. Zhukova, M. V. Melnik, A. O. Ismagilov, V. P. Chegnov, O. I. Chegnova, and A. N. Tcypkin, "Influence of iron and neodymium doping on znse crystals' optical properties studied by femtosecond pump-probe spectroscopy," *Applied Physics B*, vol. 128, no. 8, p. 154, 2022.
- [28] H. Zhao, Y. Tan, L. Zhang, R. Zhang, M. Shalaby, C. Zhang, Y. Zhao, and X.-C. Zhang, "Ultrafast hydrogen bond dynamics of liquid water revealed by terahertz-induced transient birefringence," *Light: Science & Applications*, vol. 9, no. 1, p. 136, 2020.
- [29] M. C. Hoffmann, H. Y. Hwang, N. C. Brandt, K.-L. Yeh, and K. A. Nelson, "Terahertz-induced kerr-effect in relaxor ferroelectrics," *MRS Online Proceedings Library*, vol. 1230, pp. 1–6, 2009.
- [30] S. Sarbak, G. Sharma, C. S. Joseph, W. E. Kucia, K. Dobek, R. H. Giles, and A. Dobek, "Direct observation of the thz kerr effect (tke) in deionized, distilled and buffered (pbs) water," *Physical Chemistry Chemical Physics*, vol. 19, no. 39, pp. 26749–26757, 2017.
- [31] S. Hosseini, M. Razaghi, and N. Das, "Analysis of non-linear refractive index influences on four-wave mixing conversion efficiency in semi-

- conductor optical amplifiers,” *Optics & Laser Technology*, vol. 44, no. 3, pp. 528–533, 2012.
- [32] M. L. Miguez, E. C. Barbano, S. C. Zilio, and L. Misoguti, “Accurate measurement of nonlinear ellipse rotation using a phase-sensitive method,” *Opt. Express*, vol. 22, no. 21, pp. 25 530–25 538, Oct 2014. [Online]. Available: <https://opg.optica.org/oe/abstract.cfm?URI=oe-22-21-25530>
- [33] M. L. Miguez, T. G. De Souza, E. C. Barbano, S. C. Zilio, and L. Misoguti, “Measurement of third-order nonlinearities in selected solvents as a function of the pulse width,” *Optics Express*, vol. 25, no. 4, pp. 3553–3565, 2017.
- [34] F. Novelli, “Terahertz spectroscopy of thick and diluted water solutions,” *Opt. Express*, vol. 32, no. 7, pp. 11 041–11 056, Mar 2024. [Online]. Available: <https://opg.optica.org/oe/abstract.cfm?URI=oe-32-7-11041>
- [35] M. Cornet, J. Degert, E. Abraham, and E. Freysz, “Terahertz kerr effect in gallium phosphide crystal,” *J. Opt. Soc. Am. B*, vol. 31, no. 7, pp. 1648–1652, Jul 2014. [Online]. Available: <https://opg.optica.org/josab/abstract.cfm?URI=josab-31-7-1648>
- [36] M. Zhukova, M. Melnik, I. Vorontsova, A. Tcypkin, and S. Kozlov, “Estimations of low-inertia cubic nonlinearity featured by electro-optical crystals in the thz range,” *Photonics*, vol. 7, no. 4, 2020. [Online]. Available: <https://www.mdpi.com/2304-6732/7/4/98>
- [37] S. Zibod, P. Rasekh, M. Yildirim, W. Cui, R. Bhardwaj, J.-M. Ménard, R. W. Boyd, and K. Dolgaleva, “Strong nonlinear response in crystalline quartz at thz frequencies,” *Advanced Optical Materials*, vol. 11, no. 15, p. 2202343, 2023. [Online]. Available: <https://onlinelibrary.wiley.com/doi/abs/10.1002/adom.202202343>
- [38] C. L. Korpa, G. Tóth, and J. Hebling, “Interplay of diffraction and nonlinear effects in the propagation of ultrashort pulses,” *Journal of Physics B: Atomic, Molecular and Optical Physics*, vol. 49, no. 3, p. 035401, jan 2016. [Online]. Available: <https://dx.doi.org/10.1088/0953-4075/49/3/035401>
- [39] I. Artser, M. Melnik, A. Ismagilov, M. Guselnikov, A. Tcypkin, and S. Kozlov, “Radiation shift from triple to quadruple frequency caused by the interaction of terahertz pulses with a nonlinear kerr medium,” *Scientific Reports*, vol. 12, no. 1, p. 9019, 2022.
- [40] P. L. Kramer, M. K. Windeler, K. Mecseki, E. G. Champenois, M. C. Hoffmann, and F. Tavella, “Enabling high repetition rate nonlinear thz science with a kilowatt-class sub-100 fs laser source,” *Optics Express*, vol. 28, no. 11, pp. 16 951–16 967, 2020.
- [41] T. Xia, D. Hagan, M. Sheik-Bahae, and E. Van Stryland, “Eclipsing z-scan measurement of  $\lambda/10$  4 wave-front distortion,” *Optics letters*, vol. 19, no. 5, pp. 317–319, 1994.
- [42] A. Gomes, E. Falcão Filho, C. B. de Araújo, D. Rativa, and R. De Araujo, “Thermally managed eclipse z-scan,” *Optics express*, vol. 15, no. 4, pp. 1712–1717, 2007.
- [43] V. C. Ferreira and R. R. Correia, “Characterization of thermo-optical and third-order nonlinear optical properties by eclipse i-scan,” in *Ultrafast Phenomena and Nanophotonics XXV*, vol. 11684. SPIE, 2021, pp. 13–20.
- [44] S. Mian, B. Taheri, and J. Wicksted, “Effects of beam ellipticity on z-scan measurements,” *JOSA B*, vol. 13, no. 5, pp. 856–863, 1996.
- [45] J. A. Fülöp, L. Pálfalvi, S. Klingebiel, G. Almási, F. Krausz, S. Karsch, and J. Hebling, “Generation of sub-mJ terahertz pulses by optical rectification,” *Optics Letters*, vol. 37, no. 4, p. 557, feb 2012. [Online]. Available: <https://doi.org/10.1364/FOL.37.000557>
- [46] R. W. Boyd, “Ultrafast and intense-field nonlinear optics,” *Nonlinear Optics*, pp. 561–587, 2008.
- [47] K. Ikeda, R. E. Saperstein, N. Alic, and Y. Fainman, “Thermal and kerr nonlinear properties of plasma-deposited silicon nitride/silicon dioxide waveguides,” *Opt. Express*, vol. 16, no. 17, pp. 12 987–12 994, Aug 2008. [Online]. Available: <https://opg.optica.org/oe/abstract.cfm?URI=oe-16-17-12987>